Can Cerenkov light really induce an effective photodynamic therapy?

Joël Daouk, Batoul Dhaini, Jérôme Petit, Céline Frochot, Muriel Barberi-Heyob, Hervé Schohn

radiation

MDPI

Review

Can Cerenkov Light Really Induce an Effective Photodynamic Therapy?

Joël Daouk [1], Batoul Dhaini [2], Jérôme Petit [1], Céline Frochot [2], Muriel Barberi-Heyob [1,*] and Hervé Schohn [1]

1 Centre de Recherche en Automatique de Nancy (CRAN), UMR 7039, CNRS, Université de Lorraine, Campus Santé Bât D, 9 Avenue de la Forêt de Haye, F54518 Vandoeuvre-lès-Nancy, France; joel.daouk@univ-lorraine.fr (J.D.); jerome.petit9@etu.univ-lorraine.fr (J.P.); herve.schohn@univ-lorraine.fr (H.S.)

2 Laboratoire Réactions et Génie des Procédés (LRGP), UMR 7274, CNRS, Université de Lorraine, F54000 Nancy, France; batoul.dhaini@univ-lorraine.fr (B.D.); celine.frochot@univ-lorraine.fr (C.F.)

* Correspondence: muriel.barberi-heyob@univ-lorraine.fr; Tel.: +33-372-746-114

Received: 17 October 2020; Accepted: 18 November 2020; Published: 24 November 2020

Abstract: Photodynamic therapy (PDT) is a promising therapeutic strategy for cancers where surgery and radiotherapy cannot be effective. PDT relies on the photoactivation of photosensitizers, most of the time by lasers to produced reactive oxygen species and notably singlet oxygen. The major drawback of this strategy is the weak light penetration in the tissues. To overcome this issue, recent studies proposed to generate visible light in situ with radioactive isotopes emitting charged particles able to produce Cerenkov radiation. In vitro and preclinical results are appealing, but the existence of a true, lethal phototherapeutic effect is still controversial. In this article, we have reviewed previous original works dealing with Cerenkov-induced PDT (CR-PDT). Moreover, we propose a simple analytical equation resolution to demonstrate that Cerenkov light can potentially generate a photo-therapeutic effect, although most of the Cerenkov photons are emitted in the UV-B and UV-C domains. We suggest that CR-PDT and direct UV-tissue interaction act synergistically to yield the therapeutic effect observed in the literature. Moreover, adding a nanoscintillator in the photosensitizer vicinity would increase the PDT efficacy, as it will convert Cerenkov UV photons to light absorbed by the photosensitizer.

Keywords: Cerenkov radiations; photodynamic therapy; nanoparticles; radiopharmaceuticals

1. Introduction

Photodynamic therapy (PDT) uses specific molecules, namely photosensitizing agents, photo-agents or photosensitizers (PS), along with light illumination, in the presence of oxygen, to kill cancer cells, ultimately leading to tumor eradication. PDT is also known as photoradiation therapy or photochemotherapy. PDT involves the presence of PS, light and endogenous molecular oxygen ($^3O_2$) to generate photochemical reactions. Over the past few decades, diverse synthesized PS activation by visible and near-infrared (NIR) light has been widely investigated [1]. The mechanism of PDT is based on type I and II photo-oxidation reactions. At a specific excitation wavelength (light photon absorption), the PS produces ROS causing oxidative cell damage which is highly dependent on the $^3O_2$ content within the tissue [2].

Unfortunately, due to shallow visible light penetration depth into tissues, the photodynamic therapeutic strategy currently has largely been restricted to the treatment of surface localized tumors. Additional invasive strategies, i.e., interstitial PDT, through optical fibers are currently used for getting the visible light into the intended deep-seated targets [3,4]. Indeed, compared to ionizing-radiations,

the light could not penetrate deeply because most tissue chromophores absorb in the range of the visible light spectrum commonly used in clinical practice. Moreover, the optimization of PDT modalities must consider numerous phenomena, regarding one or several main factors (photosensitizer, light, oxygen) involved in the treatment efficacy. A specific dosimetry remains challenging owing to their nonlinear interactions. Light penetration in the target tissue depends on its specific optical properties. If the tissue is hypoxic or becomes hypoxic because of the PDT treatment which consumes $^3O_2$, the yield of singlet oxygen $^1O_2$ will be lower than expected. Furthermore, making things tricky, PS concentration, light penetration and tissue oxygenation can vary during treatments and one parameter can influence the others.

To knock down the biotechnological barriers limiting the effectiveness of radiotherapy (i.e., curative X-ray dose to the tumor tissue without increasing it in the healthy adjoining tissue) and PDT (low penetration of the light), it has been proposed to use a bimodal therapy using biocompatible high-Z nanoparticles (NPs). This concept could combine both radiotherapy and PDT strategies, two clinical proven modalities, while maintaining the main benefits of each therapeutic strategy. Only PDT can generate $^1O_2$, but unfortunately, the low penetration of light remains a limiting factor. To treat deep lesions without an invasive approach, X-ray could be used as an excitation source instead of normal light. This therapeutic approach is known as X-ray-induced PDT (X-PDT) [5–9]. The light penetration limitation in the tumor tissue will be overcome and PS activation within the tumor cells will be performed by radiotherapy. This methodology requires a material composition exhibiting appropriate physical properties: high density for a good ionizing radiation interaction, high scintillation quantum yield and efficient energy transfer toward the PS as well as a biocompatibility and adapted in vivo bio-distribution. However, most of the X-PDT studies were mainly obtained with cancer cell lines or animal models bearing subcutaneous grafted cancer cells, limiting therefore clinical relevance [10]. The potential toxicity of nanoscintillators, in fact, mostly relies on nanoparticles stability, which can be enhanced by an inorganic shell among other things. As an example, AGuIX-designed nanoplatforms which originally chelate gadolinium have been assessed in phase I and phase II clinical trials without evidence of any toxicity [11,12]. AGuIX nanoparticle being a chelator, Gd3+ cations can be easily replaced by another 3+ lanthanide.

Recently, another therapeutic strategy has been proposed, direct PS activation through Cerenkov radiation, referred as Cerenkov-induced PDT (CR-PDT) [13,14]. Ran et al., in their proof-of principle article, postulated that such a treatment could be a synergy between the radiotherapeutic and phototherapeutic effect, the latter involving solely PSs activation [15]. However, despite the various recent studies demonstrating a real benefit in terms of tumor growth decrease, there is still a debate about the presence of a cytotoxic phototherapeutic effect [16]. Indeed, the number of photons absorbed by the PS being lower than those involved in PDT, the amount of $^1O_2$ produced is dramatically low.

In this article, we review the recent results obtained by researchers dealing with CR-PDT. Then, we propose an analytical assessment of $^1O_2$ production for the most used PS (photofrin) and radioisotopes used in nuclear medicine to determine whether Cerenkov radiation could produce a true phototherapeutic effect or not.

2. Cerenkov Light

Cerenkov light is a luminescence signal produced by charged particles. Two conditions must be present to enable such an effect: the medium must be dielectric and the charged particle must travel faster than the phase velocity of light in that medium. Cerenkov photons are produced by successive polarization/depolarization of the medium along the particle path, yielding constructive interferences [17]. To make it clearer, Cerenkov radiation can be compared with sound barrier crossing, but for light.

The Cerenkov photon yield can be computed with the Frank–Tamm formula [18]:

$$\frac{dN}{dx} = 2\pi\alpha(1 - \frac{1}{n^2\beta^2}) \int_{\lambda_1}^{\lambda_2} \frac{1}{\lambda^2} d\lambda, \quad (1)$$

where dN/dx is the number of photons emitted per step length; n is the refractive index of the considered medium; α is a time constant defined as 1/137; and β is the ratio between the actual particle velocity and light speed in vacuum. Only particles, where $\beta n > 1$, will be able to produce Cerenkov light. β is directly related to the particle energy following the formula:

$$\beta = \sqrt{1 - \left[\frac{1}{\left(\frac{E}{mc^2} + 1\right)}\right]^2} \quad (2)$$

Thus, to allow Cerenkov radiation, the initial particle's energy must be:

$$E > mc^2\left(\frac{1}{\sqrt{1 - n^{-2}}} - 1\right) \quad (3)$$

In biological tissues, where the refractive index is considered around 1.4, this energy threshold is around 250 keV. This threshold is much lower than most of the radionuclides emitting β^+ or β^- particles.

The Cerenkov spectrum is a continuous spectrum from UV to infra-red light where the number of photons per wavelength is proportional to $1/\lambda^2$. Cerenkov photons are not emitted isotropically from the particle, but within a cone aligned with the direction of the travelling particle. The cone aperture of the distribution (Figure 1) is related to the particle velocity as

$$\cos\theta = \frac{1}{n\beta}$$

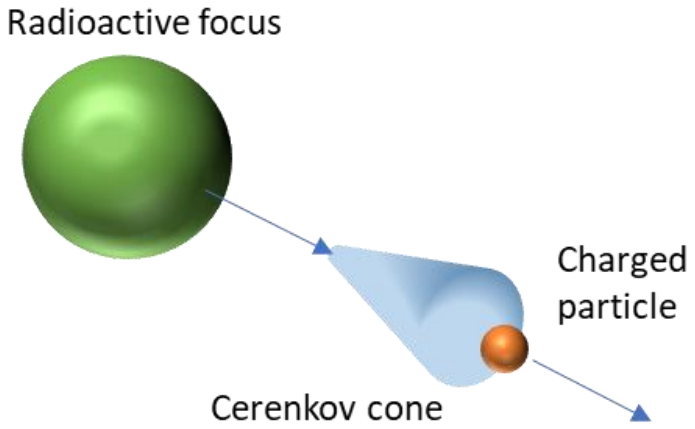

Figure 1. Illustration of Cerenkov effect in a dielectric medium. A charged particle is emitted from the radioactive focus. Its velocity in the medium is higher than light in that medium yielding Cerenkov light production in a cone. The cone orientation is colinear to particle trajectory and its aperture is defined by particle velocity. As the particle is faster than light, Cerenkov photons appear behind it.

Gill et al. highlighted the luminescence yield of several isotopes commonly used in nuclear medicine and biology [19]. They used simulations (including the true resolution of Franck–Tamm formula at each length step) to determine the quantity and spatial distribution of Cerenkov light for each assessed element. Moreover, they validated their simulation kernel by true experiments for five radionuclides covering energies from 0.611 up to 2.3 MeV. Table 1 summarizes the photon yield of the most common radionuclides used in nuclear medicine and Figure 2 presents the corresponding

Cerenkov spectra for the same isotopes. It is noteworthy that most of them are dedicated to positron emission tomography. Monte Carlo simulations assessed the spatial distribution of Cerenkov photons in biological medium. Mitchell et al. computed the volume where the charged particles energy was still higher than the Cerenkov threshold, allowing for the conclusion that many β emitters produced Cerenkov light in a 2 mm-diameter sphere [18].

Table 1. Cerenkov photon yield for main nuclear medicine elements. Data extracted from [16].

Element	Z	Halflife	Main Emission Type	Photon Yield	E_{max} (MeV)	E_{mean} (Mev)
^{11}C	6	20.4 min	b^+	6.87	0.970	0.390
^{18}F	9	110 min	b^+	1.32	0.63	0.252
^{68}Ga	31	67.7 min	b^+	33.9	1.92	0.844
^{82}Rb	37	1.27 min	b^+	80.8	3.378	1.551
^{89}Zr	40	78.4 h	b^+	2.29	0.909	0.396
^{90}Y	39	64.1 h	b^-	47.3	2.28	0.935

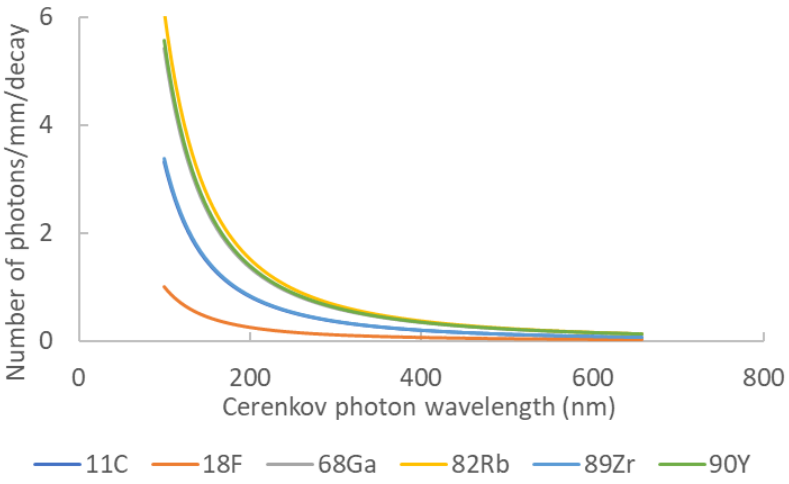

Figure 2. Cerenkov spectrum for ^{18}F, ^{68}Ga and ^{89}Zr decay in biological medium. Spectra were defined between 100 and 650 nm. To ease reading, number of photons are expressed relatively to ^{18}F at 100 nm.

3. Photosensitizer (PS) Activation Mechanisms

PS are molecules able to absorb visible light to reach an excited singlet state. Then, return to the ground state is possible following three ways: (i) non radiative deactivation, (ii) emission of a fluorescence photon, whose wavelength is higher than the absorbed photon, or (iii) formation of a triplet state. The triplet excited PS can also decay back to the ground state by non radiative deactivation or emitting phosphorescence, but most importantly it can interact directly with surrounding biological substrates: The photo oxidative reactions, namely type I reactions, lead to an electron or proton transfer to generate radicals such as superoxide, hydroxyl or hydrogen peroxide as a consequence of dismutation of superoxide. Alternatively, the energy of the excited PS can be directly transferred to $^3O_2$ (itself as a triplet in the ground state) to form $^1O_2$, corresponding to type II reaction [20]. It is worth nothing that both type I and type II reactions occur simultaneously, and the ratio between these processes is affected by the nature of the PS, as well as by the concentration of endogenous $^3O_2$ and near/adjacent biomolecules targets. However, the production of $^1O_2$ plays a dominant role in in vivo PDT efficiency with most of the PS used for clinical applications. The reactivity of $^1O_2$, through the formation of endoperoxide derivatives, with unsaturated fatty acids within membranes, cyclic amino acyl residues within protein (Histidine, Tryptophane, or Methionine), and nucleic acids (Guanosine), is the main characteristic of the photodynamic effect [21–24].

The most popular PSs used in practice are porphyrins and their derivatives. These PS present a high intensity Soret band around 400 nm and from 2 to 4 Q-bands of lower intensity up to 630 nm.

Soret band excitation is much more efficient than Q-band excitation However, UV/blue light does not penetrate deeply into tissue and red light is often used to overcome this issue. As stated before, Cerenkov radiation produce a continuous spectrum from 100 up to 650 nm following a monotonous $1/\lambda^2$ decay. Cerenkov radiation involves more UV/blue than red photons. Considering the Frank–Tamm formula, Cerenkov light should produce an infinite spectrum. In fact, high and low wavelength cut-offs can be defined: for long wavelengths (above 650~700 nm) due to medium self-absorption and for wavelengths approaching the X-ray domain (i.e., below 100 nm) [25]. However, these limitations do not interfere with the ability to activate a PS since their Soret band is classically located around 400–500 nm.

4. Cerenkov-Induced PDT Main Results

Original studies providing detailed methods and results can be separated into in vitro and in vivo works. Collectively, it has been always reported that cancer cell death is increased when PS and β emitters are associated in the same treatment protocol. A dose-dependent effect of radioactivity and PS concentrations is observed. Obviously, close co-localization of both radio-emitters and PS is required to induce an efficient therapeutic effect [26–31]. In addition, after cellular uptake, intracellular PS level is related to a significant greatest part/ratio of Cerenkov radiation [30]. However, the photodynamic effect was not observed for all the assessed cell lines. Nakamura et al. postulated that such differences could be attributed to variable radiotracer accumulation [31]. Moreover, the sensitivity to the ionizing radiations and Cerenkov light differs according to the tested cell lines. Such a direct effect leads to the decrease of the participation of CR-PDT cytotoxicity to the overall therapeutic effect. The effect of the chosen isotope has been partly evaluated by Duan et al. Even though ^{18}F-FDG was six times more incorporated in cells than ^{68}Ga-BSA, the total amount of Cerenkov photons was still higher for the latter tracer and the phototherapeutic effects were higher as well [29]. These results are consistent with the greater ^{68}Ga Cerenkov yield as compared to ^{18}F yield (33.90 vs. 1.32 photons/decay/ mm respectively).

As a consequence of the use of radionuclides, γ-H_2AX expression was studied as a marker of DNA strand break in genotoxic stress conditions γ-H_2AX is a variant sequence of histone H2A, the expression of which is often increased following a DNA strand break, and the protein localizes as foci within the nuclei. γ-H_2AX plays therefore a major role in response to DNA damage and during the initial step of the DNA repair mechanism [32]. Recently, the protein levels were found to be enhanced in breast cancer cells after cell exposure to PSs and radionuclides [27,29]. This observed increase could not be attributed solely to cell damage induced by the ionizing nature of β emitters. Indeed, Duan et al. demonstrated that cell exposure to 400 μCi of ^{68}Ga or ^{18}F alone was not associated with any γ-H_2AX nuclei focus. The same trend has been observed by Kotagiri et al. when they pointed out DNA damage in numerous fibroblasts (i.e., γ-H_2AX-induces foci), when combining PS and ^{18}F-FDG in the treatment protocol [26]. These results are consistent with the previous PDT studies which demonstrated also DNA alteration while cells did not undergo cell death [33,34]. Nevertheless, γ-H_2AX foci were not observed in all conditions. Duan et al. reported γ-H_2AX levels increase only when the PS was associated with ^{68}Ga but not with ^{18}F [29]. Similar results, such as DNA repair activation, were obtained with^{89}Zr [35], in agreement with the Cerenkov photon yield of each isotope (33.90 vs. 2.29 for ^{68}Ga and ^{89}Zr, respectively). Therefore, the PDT efficacy would not be similar considering the same radioactive deposit and PS concentration. The number of observed γ-H_2AX foci may probably be due to a cumulative effect from initial kinetic energy released by the isotope decay and PS activation. Indeed, cell exposure to ^{89}Zr isotope alone induced only a few foci compared to the treatment of both ^{89}Zr isotope and a PS [35]. Considering the $1/\lambda^2$ Cerenkov spectrum, nearly all of the produced photons are in the UV-C domain, which corresponds to the absorption area for nucleic acids (DNA and RNA) supporting the concept that Cerenkov radiation alters DNA and RNA integrity but also proteins present in the absorption range of this radiation domain. The UV-C effect is enhanced when introducing silver NPs as demonstrated by Efthekari et al. [36]. They found a significant increase of the γ H_2AX RNA levels when cells were exposed to silver NPs and UV-C compared to cells exposed

to UV-C alone. Then, they suggested a synergistic effect of UV-C and Ag NPs in altering DNA and then increasing γ H_2AX expression. At least, a great γ-H_2AX expression was associated with the generation of ROS during ^{89}Zr-induced oxidative stress [28]. The increase of ROS levels was only observed within the cells incubated with NPs bearing both the PS and the ^{89}Zr radioisotope.

In vivo assessments seem to confirm Cerenkov efficacy. Indeed, tumor progression decreased when the PS treatment was associated with isotopes. Kotagiri et al. used a HT1080 tumor model in mice. A complete tumor regression within 30 days was observed when exposing the tumor to ^{64}Cu and TiO_2 [26]. The results were all the more impressive as the tumor represented a viable hypoxic tumor model. These findings supported the concept that Cerenkov light could induce a cytotoxic phototherapeutic effect, even in a hypoxic environment. The same trend was observed with other cell lines and PS/isotope couples. As an example, the impact of a Porphyrin/^{89}Zr association on tumor development was evaluated in a mouse breast cancer model, in breast cancer cells grafted in mice. Ni et al. performed serial imaging using Cerenkov luminescence and found that the synthesized NPs remained in tumors for several days, allowing a long term PS illumination, gradual singlet oxygen production and the decrease of the tumor development, when ^{89}Zr was embedded with porphyrin into the same nanostructure [28]. Moreover, the same group highlighted an additional antiangiogenic effect [35]. Similar to the in vitro studies, the charged particle energy is a crucial point for treatment efficacy. Using TiO_2 NPs, tumor regression has been reported to be higher with ^{68}Ga decay rather than ^{18}F, despite a lower cell uptake [29]. Therefore, the co-injection of ^{68}Ga and custom TiO_2 NPs significantly inhibited tumor growth in grafted cells in a heterotopic site as compared to tumor growth in animals in the control group.

Thus, considering these various studies, Cerenkov radiation-mediated PS activation appears to be an effective phototherapeutic strategy to overcome low light penetration in tissue. Another great advantage of CR-PDT is the fact that it allows the treatment of disseminated tumors, whereas PDT or X-PDT are limited to one or a few masses due to the need of an external device [37].

Nevertheless, despite these encouraging results, there is still debate about the existence of a real phototherapeutic effect through CR-PDT [16]. To support this assertion, the authors estimated the number of hydroxyl radicals produced by a ^{18}F decay. In fact, for a positron emitted at 250 keV energy, 6800 molecules are produced through water radiolysis. Due to the TiO_2 bond, energy was too high to produce more than a few more radicals. To explain these exciting results, it has been postulated that positron could directly interact with photosensitizers, like other photocatalysts, to induce water radiolysis and then hydroxyl radicals, among other phenomena [16]. However, considering PDT efficacy through hydroxyl radical quantitation boils down to considering this therapeutic strategy like a "soft radiotherapy". The PDT effect is mainly due to $^1O_2$ production involved in type II reaction and should not be assessed through other produced ROS.

5. Singlet Oxygen Production Estimation

$^1O_2$ is generated at the site of the parent PS molecule. Due to the short diffusion distance (10–100 nm), there is a higher probability that the molecule reacts with the parent PS than with the adjacent PS molecules. Previous studies stated that the cytotoxic effect could be obtained for $^3O_2$ concentrations around 0.5 mM, that corresponds to 2×10^8 to 2×10^9 $^1O_2$ molecules per cell to be effective [38–40]. Thus, to assess whether Cerenkov photons could provide enough $^1O_2$, we propose to study, analytically, the production of $^1O_2$ for photofrin which is, at the date of preparation of this manuscript, the most clinically relevant PS, and most isotopes used in medicine.

The most used factor to predict PDT efficiency is the PDT dose, which can be expressed as the product of the light power by the PS concentration. This criterion only reflects the energy absorbed by the PS and does not consider local environment factors, such as local $^3O_2$ concentration [41,42]. Photochemical parameters are now integrated to improve dosimetry in vitro. Recent advances have provided also such information for in vivo preclinical models [43]. To assess the CR-PDT effect, we used an analytic, macroscopic model of $^1O_2$ production [44]. This model considers light diffusion,

PDT kinetics and $^3O_2$ supply terms. This model has been used in vivo and has been proven to be more predictive than PDT dose or light fluence alone [45,46].

In this model, the reaction rate equations can be expressed as [45]:

$$\frac{d[S_0]}{dt} + \left(\xi_\lambda \sigma \frac{\phi([S_0] + \delta)\left[^3O_2\right]}{\left[^3O_2\right] + \beta} \right)[S_0] = 0 \tag{4}$$

$$\frac{d\left[^3O_2\right]}{dt} + \left(\xi_\lambda \frac{\phi[S_0]}{\left[^3O_2\right] + \beta} \right)\left[^3O_2\right] - g\left(1 - \frac{\left[^3O_2\right]}{\left[^3O_2\right]_{t=0}}\right) = 0 \tag{5}$$

$$\frac{d\left[^1O_2\right]}{dt} - \left(\xi_\lambda \frac{\phi[S_0]\left[^3O_2\right]}{\left[^3O_2\right] + \beta} \right) = 0 \tag{6}$$

where $[S_0]$ is the PS concentration; ϕ, the light fluence; $[^3O_2]$, the triplet oxygen concentration; and $[^1O_2]$, the singlet oxygen concentration. ξ_λ, σ, δ, β and g are specific PS characteristics and are defined as oxygen consumption rate at wavelength λ, photobleaching ratio, low-concentration correction factor, oxygen quenching threshold concentration and macroscopic oxygen maximum perfusion rate, respectively.

In PDT, the $^3O_2$ consumption and PS photobleaching are due mainly to the high light fluence. Thus, Equations (4) and (5) cannot be ignored. On the contrary, in CR-PDT, the total number of photons emitted are dramatically lower than with an external laser source. In this condition, the $^3O_2$ consumption can reasonably be considered lower than the $^3O_2$ supply rate. Then, PS and $^3O_2$ concentrations can be considered constant during time.

The total light energy absorbed by the PS can be expressed by considering Cerenkov light as an external light source. Indeed, Cerenkov photons can be emitted in a sphere with a diameter up to 2 mm [18]. Thus, the Cerenkov fluence can be expressed as:

$$\phi_\lambda = \frac{E_\lambda . N_\lambda}{4\pi d^2}, \tag{7}$$

where E_λ is the photon energy (J) for the considered wavelength, and N_λ is the number of Cerenkov photons of the same wavelength computed by the Franck–Tamm formula in the Cerenkov light sphere having diameter d (cm).

The energy transfer cannot be considered as a Förster resonance energy transfer (FRET) phenomenon. Hence, we computed the energy absorbed per wavelength following the Beer–Lambert formula:

$$\phi_\lambda = \phi_{\lambda 0} - \phi_{\lambda 0} . e^{(\epsilon . l . c)} \tag{8}$$

where ε is the molar extension coefficient ($M^{-1} \cdot cm^{-1}$), l is the absorption length (cm) and c is the PS concentration (M).

Introducing Equation (8) in Equation (6) results in the expression of $^1O_2$ concentration production per wavelength. Thus, the total $^1O_2$ molecules produced per second and per decay can be defined as:

$$\frac{n_{^1O_2}}{dt} = \int_{\lambda_1}^{\lambda_2} \left(\xi_\lambda \frac{\left(\phi_{\lambda 0} - \phi_{\lambda 0} . e^{(\epsilon . l . c)}\right)[S_0]\left[^3O_2\right]}{\left[^3O_2\right] + \beta} \right) dt . N_A, \tag{9}$$

At last, the radioactive decay can be introduced in the latter equation to take the physical decay into consideration.

$$n_{^1O_2 t} = A_{t=0} . \int_{\lambda_1}^{\lambda_2} \left(\xi_\lambda \frac{\left(\phi_{\lambda 0} - \phi_{\lambda 0} . e^{(\epsilon . l . c)}\right)[S_0]\left[^3O_2\right]}{\left[^3O_2\right] + \beta} \right) dt . N_A . e^{\left(-\frac{\ln(2)}{T} . t\right)} \tag{10}$$

where $n_{^1O_2 t}$ is the number of $^1O_2$ at time t, $A_{t=0}$ is the initial activity and T is the physical decay time of the considered isotope.

Under these conditions, the total produced $^1O_2$ depends directly on the initial kinetic energy of the emitted particle and the isotope half-life time.

We applied Equation (10) with photofrin and various isotopes to assess the amount of $^1O_2$ produced through Cerenkov activation of the PS. PS characteristics used in this study were extracted from [45] and are summarized in Table 2.

Table 2. Photofrin photodynamic therapy (PDT) parameters used in the macroscopic PDT kinetic equations. Parameters taken from [42].

Parameter	Definition	Value
x ($cm^2 \cdot s^{-1}$;mW^{-1}) (630 nm)	Specific oxygen consumption rate	3.7×10^{-3}
$[^3O_1]$ (μM)	Triplet oxygen concentration	40
b (μM)	Oxygen quenching threshold concentration	11.9
[PS] (μM)	PS concentration	1

Figure 3 presents the $^1O_2$ production for the most common isotopes used in nuclear medicine with photofrin. For these computations, we used the β particle mean energy of each isotope and a 2-mm diameter sphere. A 10 kBq activity inside this volume is a reasonable activity which can be frequently encountered. Indeed, Kotagiri et al. estimated that a 50 mm^3 tumor could accumulate more than 1 MBq of FDG (after a 30 MBq injection). Then, a 2-mm diameter sphere represents a 5 mm^3 sphere and could contain easily up to 100 kBq, depending on the radiotracer affinity [47].

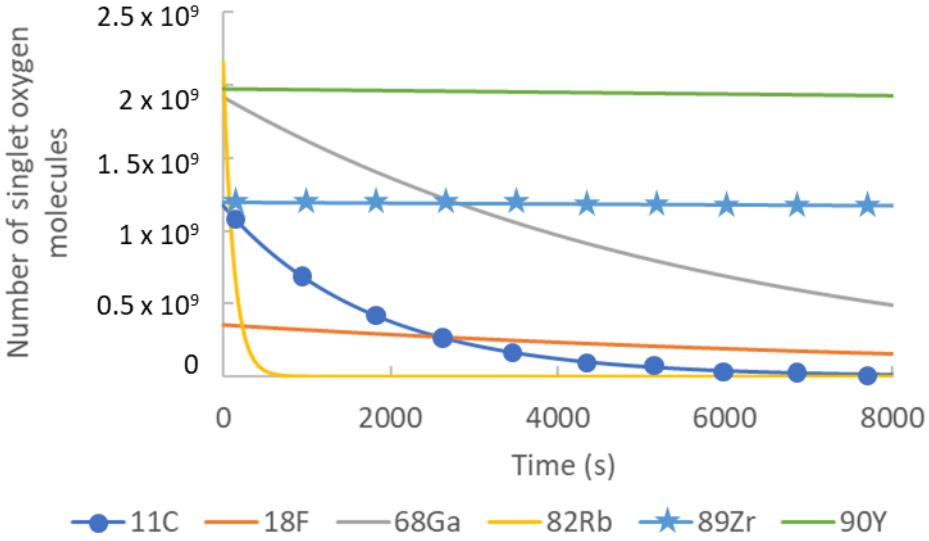

Figure 3. Dynamic singlet oxygen produced by Cerenkov photons for various isotopes. Presented curves were computed for a 2-mm diameter sphere containing 10 kBq of isotope as well as 1 μM and 40 μM of photofrin and triplet oxygen concentrations respectively.

Despite having the greatest Cerenkov yield, ^{82}Rb is the less effective $^1O_2$ producer. Indeed, its physical decay is the lowest among the isotopes (roughly 90 s). The total produced $^1O_2$ with 10 kBq ^{82}Rb was estimated at 2.71×10^{11} $^1O_2$ molecules. This is enough to destroy a hundred cancerous cells. Then, classical β^+ emitters used in positron emission tomography (i.e., ^{11}C, ^{18}F and ^{68}Ga) can produce from 2×10^{12} to 8.5×10^{12} $^1O_2$ molecules within two hours. ^{11}C and ^{18}F yield roughly the same amount of reactive oxygen species.

The main difference between them is the dynamics of $^1O_2$ production. ^{11}C has a higher Cerenkov yield than ^{18}F, but its physical lifetime is much lower (20 vs. 112 min respectively). ^{68}Ga can produce,

on average, 8.5×10^{12} $^1O_2$. As stated in previous studies, the effective threshold dose of $^1O_2$ estimated for murine breast tumor spheroids was 2×10^8 molecules per cell [40]. Similarly, a dose of 5×10^8 molecules per cell has been reported to induce liver necrosis in living rat [39]. Considering these values, the amount of $^1O_2$ produced by ^{68}Ga can destroy between 4×10^3 and 4×10^4 cancerous cells for 10 kBq associated with 1 µM of photofrin after a 2 h exposure. The most effective emitters are ^{89}Zr and ^{90}Y. Both isotopes have the longest lifetime. The amount of $^1O_2$ produced yields the destruction of 7.6×10^3 to 7.6×10^4 cells with the same radioactive concentration as before. Collectively, our estimation supported the concept that lifetime should be the most important factor to consider when CR-PDT is set-up.

6. Nanoscintillators Would Increase PDT Efficacy

This $^1O_2$ production estimation only considered the direct PS activation through Cerenkov radiation. However, an easy way to improve CR-PDT would involve using nanoscintillators in nanoparticles. Indeed, as stated before, most of the Cerenkov light is in the UV domain and many lanthanides (e.g., Terbium) has a strong UV absorption yielding a high luminescence. This strategy is similar to the X-PDT approach where X-rays are used to excite nanoscintillator which, in turn, activate PS [9]. It requires nanoparticles exhibiting appropriated physical properties to establish energy transduction from the nanoscintillator to the PS, a high scintillation quantum yield and an optimal energy transfer from the scintillator onto the PS [48,49]. However, one of the biggest X-PDT pitfall is that, only a small fraction of the X-ray emitted photons will be converted into scintillations [50]. In addition, X-PDT has been studied in preclinical conditions, with X-ray energies ranging from dozen to a few hundred keV. In a clinical context here X-ray beam is set around 6 MeV, scintillation yield is dramatically lower since the probability of photoelectric interaction becomes minimal [38]. In these conditions, it is of great interest to find another way to activate the entire system nanoscintillator/PS in clinically compatible condition. In this way, b emitters are relevant not only because they can produce Cerenkov radiation able to excite both PS and nanoscintillators; but also, for positron emitters, because the 511 keV annihilation photons can also be converted to visible light by the scintillators to offer a third PS activation way. Then, PS would be excited from both scintillating element and direct Cerenkov photons (Figure 4).

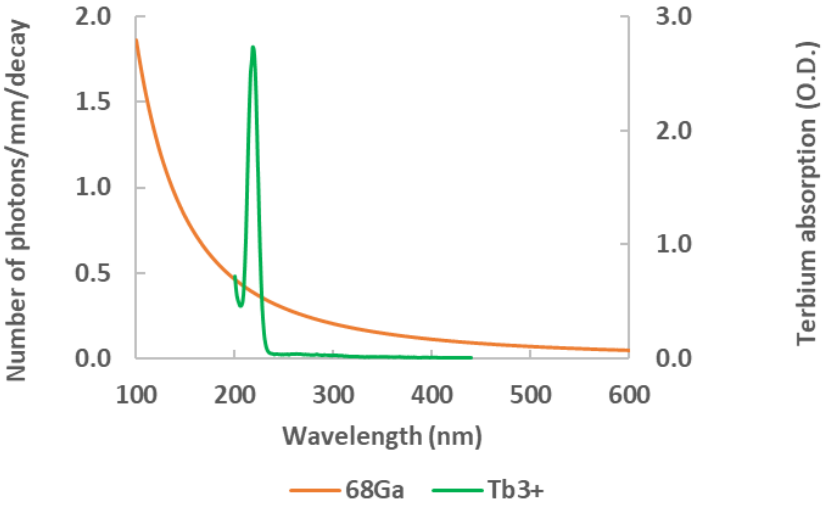

Figure 4. *Cont.*

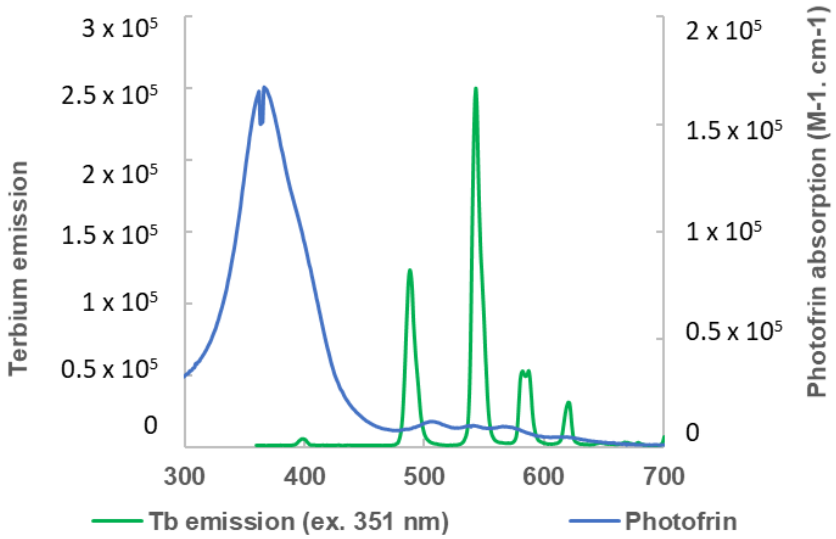

Figure 4. Up: 68Ga Cerenkov spectrum overlapping Terbium absorption spectrum (between 280 and 520 nm). Terbium presents a high absorption band around 220 nm. Bottom: Terbium emission overlapping photofrin absorption spectra. Terbium was excited with 351 nm UV source and presented 4 characteristic peaks (490, 545, 590 and 620 nm). These Terbium emission wavelengths are able to excite the photosensitizers (PS) and thus to produce photodynamic therapy (PDT) effect. Hence, Cerenkov light can both excite the PS, mostly between 350–400 nm, and the Terbium, used as a scintillator, to involve two PS activation ways.

7. Conclusions

Cerenkov light should be able to induce a PDT effect yielding cell death in tumor tissue with a minimal local radioactive concentration. The fact the greatest part of Cerenkov photons is in the UV-C domain means that this must be taken into consideration, when dealing with CR-PDT. Indeed, PSs absorb the light between 400 and 650 nm (i.e., the visible domain), suggesting that most of Cerenkov photons do not activate type II photoreactions which generate $^1O_2$. Nevertheless, UV-B and UV-C induce oxidative stress and DNA damage which trigger cell to cell death. An easy way to improve CR-PDT would be the addition of nanoscintillators to convert UV photons to wavelengths absorbed by the PS. Hence, the overall mechanism, involved in a possible synergy of direct UV and Cerenkov photon interactions, should be detailed to fully explain the observed CR-PDT efficacy.

Author Contributions: J.D. performed mathematical study B.D. contributed to photophysical aspect of the study; J.P. conducted literature review; C.F. and M.B.-H. reviewed article and strengthened PDT aspects of the paper and H.S. contributed to literature review. All the authors contributed to the original draft redaction. All authors have read and agreed to the published version of the manuscript.

Funding: This research received no external funding.

Acknowledgments: The authors wish to thank Simon Thornton (New Zealand) for reviewing the English and for advice on this article.

Conflicts of Interest: The authors declare no conflict of interest.

References

1. Niedre, M.; Patterson, M.S.; Wilson, B.C. Direct near-infrared luminescence detection of singlet oxygen generated by photodynamic therapy in cells in vitro and tissues in vivo. *Photochem. Photobiol.* **2002**, *75*, 382–391. [CrossRef]
2. Hirschberg, H.; Berg, K.; Peng, Q. Photodynamic therapy mediated immune therapy of brain tumors. *Neuroimmunol. Neuroinflamm.* **2018**, *5*, 27. [CrossRef] [PubMed]

3. Gill, I.S.; Azzouzi, A.-R.; Emberton, M.; Coleman, J.A.; Coeytaux, E.; Scherz, A.; Scardino, P.T.; PCM301 Study Group. Randomized Trial of Partial Gland Ablation with Vascular Targeted Phototherapy versus Active Surveillance for Low Risk Prostate Cancer: Extended Followup and Analyses of Effectiveness. *J. Urol.* **2018**, *200*, 786–793. [CrossRef] [PubMed]
4. Bechet, D.; Mordon, S.R.; Guillemin, F.; Barberi-Heyob, M.A. Photodynamic therapy of malignant brain tumours: A complementary approach to conventional therapies. *Cancer Treat. Rev.* **2014**, *40*, 229–241. [CrossRef] [PubMed]
5. Chen, W.; Zhang, J. Using Nanoparticles to Enable Simultaneous Radiation and Photodynamic Therapies for Cancer Treatment. *J. Nanosci. Nanotechnol.* **2006**, *6*, 1159–1166. [CrossRef] [PubMed]
6. Popovich, K.; Tomanova, K.; Čuba, V.; Procházková, L.; Pelikánová, I.T.; Jakubec, I.; Mihóková, E.; Nikl, M. LuAG:Pr3+-porphyrin based nanohybrid system for singlet oxygen production: Toward the next generation of PDTX drugs. *J. Photochem. Photobiol. B Biol.* **2018**, *179*, 149–155. [CrossRef] [PubMed]
7. Chen, M.-H.; Jenh, Y.-J.; Wu, S.-K.; Chen, Y.-S.; Hanagata, N.; Lin, F.-H. Non-invasive Photodynamic Therapy in Brain Cancer by Use of Tb3+-Doped LaF3 Nanoparticles in Combination with Photosensitizer Through X-ray Irradiation: A Proof-of-Concept Study. *Nanoscale Res. Lett.* **2017**, *12*, 1–6. [CrossRef]
8. Bulin, A.-L.; Truillet, C.; Chouikrat, R.; Lux, F.; Frochot, C.; Amans, D.; LeDoux, G.; Tillement, O.; Perriat, P.; Barberi-Heyob, M.; et al. X-ray-Induced Singlet Oxygen Activation with Nanoscintillator-Coupled Porphyrins. *J. Phys. Chem. C* **2013**, *117*, 21583–21589. [CrossRef]
9. LaRue, L.; Ben Mihoub, A.; Youssef, Z.; Colombeau, L.; Acherar, S.; André, J.-C.; Arnoux, P.; Baros, F.; Vermandel, M.; Frochot, C. Using X-rays in photodynamic therapy: An overview. *Photochem. Photobiol. Sci.* **2018**, *17*, 1612–1650. [CrossRef]
10. Sun, W.; Zhou, Z.; Pratx, G.; Chen, X.; Chen, H. Nanoscintillator-Mediated X-Ray Induced Photodynamic Therapy for Deep-Seated Tumors: From Concept to Biomedical Applications. *Theranostics* **2020**, *10*, 1296–1318. [CrossRef]
11. Verry, C.; Sancey, L.; Dufort, S.; Le Duc, G.; Mendoza, C.; Lux, F.; Grand, S.; Arnaud, J.; Quesada, J.L.; Villa, J.; et al. Treatment of multiple brain metastases using gadolinium nanoparticles and radiotherapy: NANO-RAD, a phase I study protocol. *BMJ Open* **2019**, *9*, e023591. [CrossRef] [PubMed]
12. Verry, C.; Dufort, S.; Lemasson, B.; Grand, S.; Pietras, J.; Troprès, I.; Crémillieux, Y.; Lux, F.; Mériaux, S.; Larrat, B.; et al. Targeting brain metastases with ultrasmall theranostic nanoparticles, a first-in-human trial from an MRI perspective. *Sci. Adv.* **2020**, *6*, eaay5279. [CrossRef] [PubMed]
13. Dothager, R.S.; Goiffon, R.J.; Jackson, E.; Harpstrite, S.; Piwnica-Worms, D. Cerenkov Radiation Energy Transfer (CRET) Imaging: A Novel Method for Optical Imaging of PET Isotopes in Biological Systems. *PLoS ONE* **2010**, *5*, e13300. [CrossRef] [PubMed]
14. Liu, H.; Zhang, X.; Xing, B.; Han, P.; Gambhir, S.S.; Cheng, Z. Radiation-Luminescence-Excited Quantum Dots for in vivo Multiplexed Optical Imaging. *Small* **2010**, *6*, 1087–1091. [CrossRef] [PubMed]
15. Ran, C.; Zhang, Z.; Hooker, J.M.; Moore, A. In Vivo Photoactivation Without "Light": Use of Cherenkov Radiation to Overcome the Penetration Limit of Light. *Mol. Imaging Biol.* **2012**, *14*, 156–162. [CrossRef]
16. Pratx, G.; Kapp, D.S. Is Cherenkov luminescence bright enough for photodynamic therapy? *Nat. Nanotechnol.* **2018**, *13*, 354. [CrossRef]
17. Jelley, J.V. *Cherenkov Radiation and Its Applications*; Pergamon Press: London, UK, 1958; p. 314.
18. Mitchell, G.S.; Gill, R.K.; Boucher, D.L.; Li, C.; Cherry, S.R. In vivo Cerenkov luminescence imaging: A new tool for molecular imaging. *Philos. Trans. R. Soc. A.* **2011**, *369*, 4605–4619. [CrossRef]
19. Gill, R.K.; Mitchell, G.S.; Cherry, S.R. Computed Cerenkov luminescence yields for radionuclides used in biology and medicine. *Phys. Med. Biol.* **2015**, *60*, 4263–4280. [CrossRef]
20. Moan, J.; Berg, K. The photodegradation of porphyrins in cells can be used to estimate the lifetime of singlet oxygen. *Photochem. Photobiol.* **1991**, *53*, 549–553. [CrossRef]
21. Calixto, G.M.F.; Bernegossi, J.; De Freitas, L.M.; Fontana, C.R.; Chorilli, M. Nanotechnology-Based Drug Delivery Systems for Photodynamic Therapy of Cancer: A Review. *Molecules* **2016**, *21*, 342. [CrossRef]
22. Karunakaran, S.C.; Babu, P.S.S.; Madhuri, B.; Marydasan, B.; Paul, A.K.; Nair, A.S.; Rao, K.S.; Srinivasan, A.; Chandrashekar, T.K.; Rao, C.M.; et al. In VitroDemonstration of Apoptosis Mediated Photodynamic Activity and NIR Nucleus Imaging through a Novel Porphyrin. *ACS Chem. Biol.* **2013**, *8*, 127–132. [CrossRef] [PubMed]

23. Liu, K.; Liu, X.; Zeng, Q.; Zhang, Y.; Tu, L.; Liu, T.; Kong, X.; Wang, Y.; Cao, F.; Lambrechts, S.A.G.; et al. Covalently Assembled NIR Nanoplatform for Simultaneous Fluorescence Imaging and Photodynamic Therapy of Cancer Cells. *ACS Nano* **2012**, *6*, 4054–4062. [CrossRef] [PubMed]
24. Sharman, W.M.; Allen, C.M.; Van Lier, J.E. Photodynamic therapeutics: Basic principles and clinical applications. *Drug Discov. Today* **1999**, *4*, 507–517. [CrossRef]
25. Ciarrocchi, E.; Belcari, N. Cerenkov luminescence imaging: Physics principles and potential applications in biomedical sciences. *EJNMMI Phys.* **2017**, *4*, 14. [CrossRef] [PubMed]
26. Kotagiri, N.; Sudlow, G.P.; Akers, W.J.; Achilefu, S. Breaking the depth dependency of phototherapy with Cerenkov radiation and low-radiance-responsive nanophotosensitizers. *Nat. Nanotechnol.* **2015**, *10*, 370–379. [CrossRef] [PubMed]
27. Kamkaew, A.; Cheng, L.; Goel, S.; Valdovinos, H.F.; Barnhart, T.E.; Liu, Z.; Cai, W. Cerenkov Radiation Induced Photodynamic Therapy Using Chlorin e6-Loaded Hollow Mesoporous Silica Nanoparticles. *ACS Appl. Mater. Interfaces* **2016**, *8*, 26630–26637. [CrossRef] [PubMed]
28. Ni, D.; Ferreira, C.A.; Barnhart, T.E.; Quach, V.; Yu, B.; Jiang, D.; Wei, W.; Liu, H.; Engle, J.W.; Hu, P.; et al. Magnetic Targeting of Nanotheranostics Enhances Cerenkov Radiation-Induced Photodynamic Therapy. *J. Am. Chem. Soc.* **2018**, *140*, 14971–14979. [CrossRef]
29. Duan, D.; Liu, H.; Xu, Y.; Han, Y.; Xu, M.; Zhang, Z.; Liu, Z. Activating TiO_2 Nanoparticles: Gallium-68 Serves as a High-Yield Photon Emitter for Cerenkov-Induced Photodynamic Therapy. *ACS Appl. Mater. Interfaces* **2018**, *10*, 5278–5286. [CrossRef]
30. Hartl, B.A.; Hirschberg, H.; Marcu, L.; Cherry, S.R. Activating Photodynamic Therapy in vitro with Cerenkov Radiation Generated from Yttrium-90. *J. Environ. Pathol. Toxicol. Oncol.* **2016**, *35*, 185–192. [CrossRef]
31. Nakamura, Y.; Nagaya, T.; Sato, K.; Okuyama, S.; Ogata, F.; Wong, K.J.; Adler, S.; Choyke, P.L.; Kobayashi, H. Cerenkov Radiation–Induced Photoimmunotherapy with 18F-FDG. *J. Nucl. Med.* **2017**, *58*, 1395–1400. [CrossRef]
32. Ivashkevich, A.; Redon, C.E.; Nakamura, A.J.; Martin, R.F.; Martin, O.A. Use of the γ-H2AX assay to monitor DNA damage and repair in translational cancer research. *Cancer Lett.* **2012**, *327*, 123–133. [CrossRef] [PubMed]
33. Robertson, C.A.; Evans, D.H.; Abrahamse, H. Photodynamic therapy (PDT): A short review on cellular mechanisms and cancer research applications for PDT. *J. Photochem. Photobiol. B Biol.* **2009**, *96*, 1–8. [CrossRef] [PubMed]
34. Baldea, I.; Olteanu, D.; Bolfa, P.; Tăbăran, A.-F.; Ion, R.-M.; Filip, G.A. Melanogenesis and DNA damage following photodynamic therapy in melanoma with two meso-substituted porphyrins. *J. Photochem. Photobiol. B Biol.* **2016**, *161*, 402–410. [CrossRef] [PubMed]
35. Yu, B.; Ni, D.; Rosenkrans, Z.T.; Barnhart, T.E.; Wei, H.; Ferreira, C.A.; Lan, X.; Engle, J.W.; He, Q.; Yu, F.; et al. A "Missile-Detonation" Strategy to Precisely Supply and Efficiently Amplify Cerenkov Radiation Energy for Cancer Theranostics. *Adv. Mater.* **2019**, *31*, e1904894. [CrossRef]
36. Eftekhari-Kenzerki, Z.; Fardid, R.; Behzad-Behbahani, A. Impact of Silver Nanoparticles on the Ultraviolet Radiation Direct and Bystander Effects on TK6 Cell Line. *J. Med. Phys.* **2019**, *44*, 118–125.
37. Kotagiri, N.; Cooper, M.L.; Rettig, M.; Egbulefu, C.; Prior, J.; Cui, G.; Karmakar, P.; Zhou, M.; Yang, X.; Sudlow, G.; et al. Radionuclides transform chemotherapeutics into phototherapeutics for precise treatment of disseminated cancer. *Nat. Commun.* **2018**, *9*, 1–12. [CrossRef]
38. Clement, S.; Deng, W.; Camilleri, E.; Wilson, B.C.; Goldys, E.M. X-ray induced singlet oxygen generation by nanoparticle-photosensitizer conjugates for photodynamic therapy: Determination of singlet oxygen quantum yield. *Sci. Rep.* **2016**, *6*, 19954. [CrossRef]
39. Farrell, T.J.; Wilson, B.C.; Patterson, M.S.; Chow, R. Dependence of photodynamic threshold dose on treatment parameters in normal rat liver in vivo. In Proceedings of the Optics, Electro-Optics, and Laser Applications in Science and Engineering, Los Angeles, CA, USA, 1 June 1991.
40. Georgakoudi, I.; Nichols, M.G.; Foster, T.H. The Mechanism of Photofrin Photobleaching and Its Consequences for Photodynamic Dosimetry. *Photochem. Photobiol.* **1997**, *65*, 135–144. [CrossRef]
41. Rizvi, I.; Anbil, S.; Alagic, N.; Celli, J.P.; Zheng, L.Z.; Palanisami, A.; Glidden, M.D.; Pogue, B.W.; Hasan, T. PDT dose parameters impact tumoricidal durability and cell death pathways in a 3D ovarian cancer model. *Photochem. Photobiol.* **2013**, *89*, 942–952. [CrossRef]
42. Penjweini, R.; Liu, B.; Kim, M.M.; Zhu, T.C. Explicit dosimetry for 2-(1-hexyloxyethyl)-2-devinyl pyropheophorbide-a-mediated photodynamic therapy: Macroscopic singlet oxygen modeling. *J. Biomed. Opt.* **2015**, *20*, 128003. [CrossRef]

43. Kim, M.M.; Ghogare, A.A.; Greer, A.; Zhu, T.C. On thein vivophotochemical rate parameters for PDT reactive oxygen species modeling. *Phys. Med. Biol.* **2017**, *62*, R1–R48. [CrossRef] [PubMed]
44. Wang, K.K.-H.; Finlay, J.C.; Busch, T.M.; Hahn, S.M.; Zhu, T.C. Explicit dosimetry for photodynamic therapy: Macroscopic singlet oxygen modeling. *J. Biophotonics* **2010**, *3*, 304–318. [CrossRef] [PubMed]
45. Qiu, H.; Kim, M.M.; Penjweini, R.; Zhu, T.C. Macroscopic singlet oxygen modeling for dosimetry of Photofrin-mediated photodynamic therapy: An in-vivo study. *J. Biomed. Opt.* **2016**, *21*, 88002. [CrossRef] [PubMed]
46. Qiu, H.; Kim, M.M.; Penjweini, R.; Finlay, J.C.; Busch, T.M.; Wang, T.; Guo, W.; Cengel, K.A.; Simone, C.B.; Glatstein, E.; et al. A Comparison of Dose Metrics to Predict Local Tumor Control for Photofrin-mediated Photodynamic Therapy. *Photochem. Photobiol.* **2017**, *93*, 1115–1122. [CrossRef] [PubMed]
47. Kotagiri, N.; Laforest, R.; Achilefu, S. Reply to Is Cherenkov luminescence bright enough for photodynamic therapy? *Nat. Nanotechnol.* **2018**, *13*, 354–355. [CrossRef]
48. Kamkaew, A.; Chen, F.; Zhan, Y.; Majewski, R.L.; Cai, W. Scintillating Nanoparticles as Energy Mediators for Enhanced Photodynamic Therapy. *ACS Nano* **2016**, *10*, 3918–3935. [CrossRef]
49. Zou, X.; Yao, M.; Ma, L.; Hossu, M.; Han, X.; Juzenas, P.; Chen, W. X-ray-induced nanoparticle-based photodynamic therapy of cancer. *Nanomedicine* **2014**, *9*, 2339–2351. [CrossRef]
50. Ren, X.-D.; Hao, X.-Y.; Li, H.-C.; Ke, M.-R.; Zheng, B.-Y.; Huang, J. Progress in the development of nanosensitizers for X-ray-induced photodynamic therapy. *Drug Discov. Today* **2018**, *23*, 1791–1800. [CrossRef]